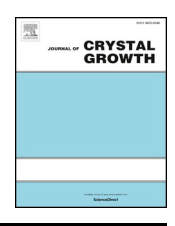


Contents lists available at ScienceDirect

Journal of Crystal Growth

journal homepage: www.elsevier.com/locate/jcrysgro



Low background doping in AlInN grown on GaN via metalorganic vapor phase epitaxy



Damir Borovac¹, Wei Sun¹, Matthew R. Peart, Renbo Song, Jonathan J. Wierer Jr., Nelson Tansu

Center for Photonics and Nanoelectronics, Department of Electrical and Computer Engineering, Lehigh University, Bethlehem, PA 18015, USA

ARTICLE INFO

Communicated by T. Paskova

Keywords:

A1. Characterization

A1. Charact

A3. Metalorganic vapor phase epitaxy

B1. Nitrides

B2. Semiconducting materials

ABSTRACT

Nearly lattice-matched and unintentionally doped AlInN films with low background doping grown via metalorganic vapor phase epitaxy on GaN/sapphire are investigated. The lattice-matched condition is verified with x-ray diffraction (XRD), and the films exhibit typical morphological characteristics for AlInN. The optical constants (n_r & k) and thicknesses of the AlInN films are determined via spectroscopic ellipsometry, finding an $n_r \sim 2.2$ at 500 nm and a bandgap of \sim 4.366 eV. Temperature-dependent Hall measurements in the Van der Pauw configuration are performed for temperatures from 80 K up to 350 K, and a low background doping concentration ($n \sim 3 \times 10^{17}$ cm $^{-3}$) and high electron mobility ($\mu_e \sim 320$ cm 2 /V·s) are found at room temperature. Simulations are performed to determine the influence of the 2-D electron gas (2DEG) caused by polarization fields from the GaN/AlInN interface and validate the Hall measurements. Thus, this work shows the potential of achieving high-quality AlInN films with low background doping densities for use in power electronic devices and deep-ultraviolet light-emitting diodes.

1. Introduction

III-nitride semiconductors are a leading material platform for next generation of devices because of their ability to tune the energy band gap from 0.7 eV (InN) up to 6.2 eV (AlN), along with their high thermal, chemical and mechanical stability [1–3]. Its largest impact is in the field of solid-state lighting, where the Nobel Prize in Physics was awarded in 2014 for advances in blue light-emitting diodes [4]. Recent advances have also demonstrated, with one more recent development of using GaN to replace Si-based power devices [5]. In addition to GaN for power devices, other ultrawide bandgap (UWBG) semiconductors like AlGaN, BN and $\beta\text{-Ga}_2\text{O}_3$ are sought out due to their ability of achieving high electric fields before impact ionization, leading to a high-power figure-of-merit (FOM). UWBG semiconductors do have challenges though, such as the difficulty of achieving p-type doping in $\beta\text{-Ga}_2\text{O}_3$ [6] and no suitable lattice-matched substrates for high Alcontent AlGaN [5].

The ternary $Al_xIn_{1-x}N$ alloys are also part of the UWBG family with a similar power FOM to β -Ga₂O₃ and AlGaN [19]. The strain state (tensile or compressive) can be controlled when grown on GaN substrates, and when $x \sim 0.83$, it is lattice-matched to GaN. Lattice matched growth of AlInN to GaN has led to high-quality distributed Bragg reflectors (DBRs) [7], cladding layers in laser diodes [8], photodetectors [9], high-

mobility field-effect transistors [10,11], electron barrier layers in InGaN-based light-emitting diodes [12], and thermoelectricity applications [13,14]. In addition, AlInN films can be p- and n-type doped [15,16], can be oxidized [17], have high thermal stability [18] and possess a large energy band gap (~4.4 eV) when grown lattice-matched to GaN [7]. We recently proposed the use of AlInN in vertical power devices [19]. Therefore, the advantageous material properties of AlInN coupled with the potential innovative device design warrant further investigations.

Despite extensive research efforts devoted to understanding the growth mechanisms of high-quality "thick" (> 300 nm) AlInN, achieving low background doping densities is a significant challenge [14,15,20,21]. AlInN films grown via metalorganic vapor phase epitaxy (MOVPE) require a relatively low growth temperature (~800 °C) in order to achieve the proper In-content when lattice matched to GaN. Growth at these temperatures can result in the incorporation of carbon and oxygen impurities into the film [14,15,22] and have high background doping concentrations on the order of $\sim\!10^{18}\text{--}10^{19}~\text{cm}^{-3}$ [14,15,23]. Thus, reducing the background doping concentration and realizing thick AlInN layers are exciting challenges that will enable the use of AlInN as p-type layers and drift layers in power electronics devices.

In this work, we report on the recently improved growth conditions

E-mail addresses: dab315@lehigh.edu (D. Borovac), tansu@lehigh.edu (N. Tansu).

 $^{^{1}}$ The authors contributed equally to this work.

of unintentionally doped, nearly lattice-matched $Al_xIn_{1-x}N$ (x ~ 0.82) films grown via MOVPE on top of GaN on sapphire templates. The structural and morphological characteristics of the Al_{0.82}In_{0.18}N film is determined by x-ray diffraction (XRD) and atomic force microscopy (AFM). Spectroscopic ellipsometry (SE) measurements are employed to estimate the thickness of the AlInN film at ~275 nm, and evaluate its optical constants (refractive indices, n_r and extinction coefficients, k). Temperature-dependent Hall measurements for temperatures from 80 K up to 350 K are performed in the Van der Pauw configuration to obtain the electron concentration (n) and mobility (μ_n) of the AlInN film. The Hall measurements at room temperature reveal that $n \sim 3 \times 10^{17}/\text{cm}^3$ and $\mu_n \sim 320 \text{ cm}^2/\text{V}$ ·s. In addition, simulations are performed to determine the influence of the 2D electron gas (2DEG) on the electron concentration arising from the polarization-induced electric field at the AlInN/GaN interface and validate the Hall measurements. Finally, impurities such as oxygen and carbon that effect the overall electron concentration are determined from secondary-ion mass spectroscopy (SIMS). This data suggests the promising potential of lowering the background doping density of nearly lattice-matched AlInN to GaN, which has profound impact on the potential integration of AlInN films in III-nitride-based power electronic devices and laser diodes.

2. Experimental methods

The AlInN films are grown on top of an unintentionally-doped GaN (u-GaN) template on sapphire substrate in a Veeco P75 MOVPE reactor. Ammonia (NH₃) is the group-V precursor, and the group-III precursors are trimethylgallium (TMGa), trimethylaluminum (TMAl) and trimethylindium (TMIn). The $\sim 3~\mu m$ thick u-GaN template is grown first and separately by employing an etch-back and recovery process with a low-temperature (~30 nm) GaN buffer layer, followed by the hightemperature GaN layer grown at T ~ 1050 °C. Then, to obtain the lattice-matched condition, the AlInN samples are grown at a pressure of 75 Torr and a temperature of ~790 °C, with the metalorganic (MO) delivery flow rates (moles/min) adjusted to produce a TMIn/TMAl molar ratio of \sim 1.65. The In-content is determined by performing XRD scans in the (002) direction and fitted by using the X'Pert Epitaxy software assuming a fully strained AlInN layer [18]. The AFM images are obtained using a Veeco Dimension 5000 and the Hall measurements are carried out using the Ecopia HMS5500 measurement system in the Van der Pauw configuration. For the Hall measurement, the samples are prepared by cutting into squares that are 10 mm × 10 mm, and indium is deposited at the corners and annealed at T = 250 °C which resulted in Ohmic contacts.

3. Results and discussion

Fig. 1(a) shows the XRD $\omega/2\theta$ (002) scan of the Al_{0.82}In_{0.18}N film grown nearly lattice-matched to GaN. Two distinct peaks are observed, with the GaN peak on the left and the Al_{0.82}In_{0.18}N peak on the righthand side. The full-width at half-maximum (FWHM) of the AlInN peak is ~275 arcsec and no additional peaks or shoulders are observed. Moreover, the inset of Fig. 1(a) shows the XRD reciprocal space map (RSM) scan obtained in the (1 0 $\bar{1}$ 5) direction. The vertical dashed line is drawn to illustrate the pseudomorphic nature of the AlInN film and indicate the film is nearly lattice-matched (or pseudomorphic) to GaN. Fig. 1(b) shows the AFM (1 μ m × 1 μ m) scan of the ~275 nm AlInN sample and a relatively rough surface is observed. It should be noted that the surface is relatively smooth between the areas with creases and large pits, which has been observed in AlInN films that exceed thicknesses of 100 nm [20,21]. A root-mean-square (RMS) roughness of ~3.41 nm is found and the value is in good agreement with those reported by Miyoshi et al. [21]. The surface contains several V-defectrelated dislocations, as is common for AlInN alloys grown on GaN (on sapphire), and are a result of propagating dislocations which arise from the underlying GaN layer [24]. They are strain related [25] or originate from kinetics-related phenomena [20]. In addition, it is observed that the top surface exhibits a granular morphology suggesting the sample is grown under slight compressive strain [21] as the In-content (~18%) is slightly higher than the lattice-matched condition (\sim 16.6%) [21], and has thus resulted in a lattice strain (ε_{xx}) of -0.28%.

Fig. 2 shows the refractive index (n_r) and extinction coefficient (k)for the $Al_{0.82}In_{0.18}N$ film in a wavelength range from 250 nm to 800 nm determined by SE. The n_r and k values are obtained through measurements of the complex reflectance ratio which is parameterized by an amplitude ratio ψ and a phase difference Δ for angles of 40°, 55° and 70°, and then fitted via the Tauc-Lorentz oscillator model [19]. For comparison purposes, the n_r and k of an Al_{0.825}In_{0.175}N (~80 nm) film from Aschenbrenner et al. [26] are plotted as well. The values for the extinction coefficient are in good agreement with previous results [26], while the refractive indices deviate from each other beyond 600 nm. The small discrepancies in the values can be attributed to the difference in the In-content (\sim 0.5%) and the difference in the thicknesses of the two films. In particular, our film is ~3.5 times thicker than that in Ref. [26] and it has been reported that variations in the In-content during the growth of thick (> 100 nm) AlInN films can be severe [20], which may be the cause of the observed differences, due to averaging effects from the SE measurements. Additionally, in the works of Aschenbrenner et al. [26], an annealing step was performed after the growth of the AlInN layer, which may cause a roughening of the top-most surface due to In-desorption [18,26]. Moreover, the SE data is used to extract the absorption coefficient $(\alpha E)^2$, as shown in the insert in Fig. 2. The

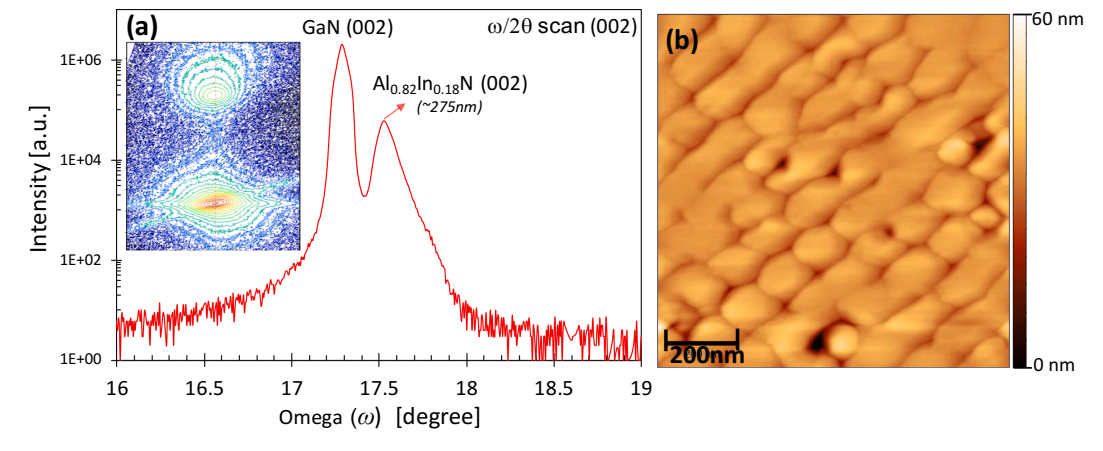


Fig. 1. . (a) XRD $\omega/2\theta$ (002) scan of the Al $_{0.18}$ In $_{0.82}$ N (\sim 275 nm) sample grown on GaN on sapphire, and (b) an AFM (1 μ m \times 1 μ m) scan of the sample with an RMS roughness of \sim 3.41 nm. The insert in (a) is the reciprocal space map scan in the (1 0 $\bar{1}$ 5) direction.

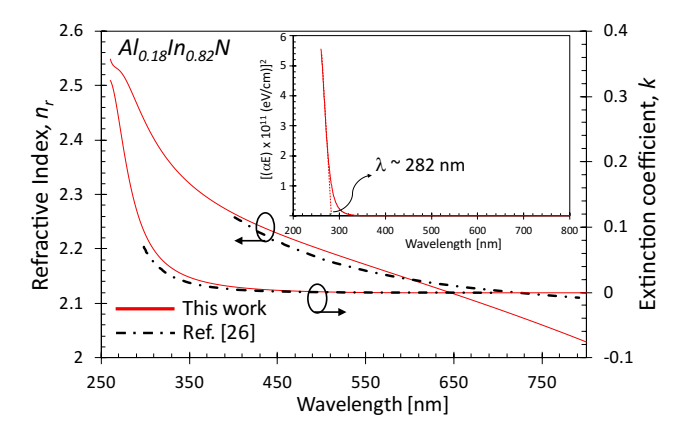


Fig. 2. . Refractive index (n_r) and extinction coefficient (k) as a function of wavelength for the $Al_{0.82}In_{0.18}N$ sample measured via spectroscopic ellipsometry. Data from Aschenbrenner et al. (Ref. [25]) for an $Al_{0.825}In_{0.175}N$ sample is also plotted for reference purposes.

dashed line in the insert is drawn as a tangent to the absorption curve and it intersects at a wavelength of 284 nm, indicating that the energy bandgap of the sample is \sim 4.366 eV, similar to previous works [7].

Fig. 3(a) shows the *n* measured by Hall of the unintentionally-doped AlInN film at temperatures ranging from 80 K to 350 K. At room temperature it is n-type with a background doping electron concentration $n \sim 3 \times 10^{17} \text{ cm}^{-3}$, which is lower by nearly an order of magnitude compared to previously reported values ($n \sim 2 \times 10^{18} \text{ cm}^{-3}$). A decrease by an order of magnitude compared to previous results is a significant step towards the potential integration of AlInN in power devices and realization of p-type doped AlInN layers suitable for DUV applications [15,19] and may indicate that there is further improvement possible with additional growth optimization. The behavior of the electron concentration versus temperature are "textbook" and observed in Fig. 3(a), with an intrinsic region at high temperatures (1000/ T < 5), a saturation region at mid-range temperatures, and lastly a freeze-out region at the lowest temperatures (1000/T > 9). Furthermore, Fig. 3(b) shows the electron mobility as a function of temperature for the AlInN film, for temperatures from 80 K to 350 K. The mobility peaks at ~170 K (μ_n ~ 820 cm²/V·s) and is μ_n ~ 320 cm²/V·s at room temperature. The mobilities drop at higher temperatures as expected due to the influence of non-polar optical phonon scattering, while at lower temperatures the impurity scattering limits the maximum mobility [27]. Thus, our optimized growth conditions for obtaining AlInN films grown on u-GaN (on sapphire) result in a high electron mobility and very low background doping density, which are essential material properties for enabling the use of AlInN in next-generation power

devices.

It is important to determine if the strong polarization-induced electric fields and resulting 2-dimensional electron gas (2DEG) at the GaN/AlInN interface affects the Hall measurements. Sztein et al. [28] have shown that "thick" (~280 nm) n-type AlInN films can be reliably measured using Hall measurements in the Van der Pauw configuration, as the effect of the high mobility 2D electron gasses (2DEG) are minimal. However, the Hall measurements of the AlInN film in this study have lower electron concentrations with less carrier screening, and therefore a computational analysis is performed to confirm that the electron concentrations are, in fact, unperturbed from the 2DEG effects. Typically, other groups have performed current-voltage (C-V) measurements [15,30] to determine carrier concentrations in unintentionally doped and doped (p or n) AlInN films. Here, we show that the carrier concentration can still be extracted using the Hall measurement technique under certain conditions.

To verify our Hall measurements, the AlInN on GaN structure is simulated using Silvaco Atlas TCAD software using best known values for GaN and AlInN [31]. The inset in Fig. 4(a) shows the simulated structure, where a GaN (5 µm) layer is on top of c-plane sapphire and is followed by a ~275 nm Al_{0.82}In_{0.18}N layer and air. The structure is simulated with and without the polarization-induced 2DEG to determine the error this additional conductivity causes in the determination of n. Fig. 4(a) shows a diagram of the actual n versus the measured n. In particular, the dashed line in Fig. 4(a) represents the ideal case, where the effect of the 2DEG is entirely negligible, allowing for the direct determination of the carrier concentration from the Hall measurement. The simulation (solid line) indicates that at n below $\sim 10^{17}$ cm⁻³, the measured *n* deviates substantially from the actual *n*, deeming the Hall measurement as unreliable. Fig. 4(a) plots the actual versus measured electron concentration and presents a guide for estimating the error in the Hall-measured data for films of similar thicknesses. Thus, it is possible to estimate the corrected $(n_{e,c})$ value for the electron concentration, which in our case would modify the measured values by roughly ~3–4%, and give a value of $n_{e,c} \sim 3.15 \times 10^{17}$ cm⁻³. In Fig. 4(b), a band diagram of the simulated structure is shown, where E_C and E_V represent the conduction and valence band edges, respectively. In this case, $n \sim 2 \times 10^{17}$ cm⁻³ is chosen to closely mimic that of the grown structure. The 2DEG is present at the interface, although a large fraction of the AlInN layer that is responsible for most of the conduction has flat bands. Therefore, at this electron concentration the Hall measurements are reasonably accurate for this this specific struc-

Growing AlInN films on GaN on sapphire leads to the generation of V-defects due to threading dislocations that propagate from the underlying GaN layer. As the AlInN film thickness increases, these defects allow for incorporation of oxygen and other impurities into the film. By

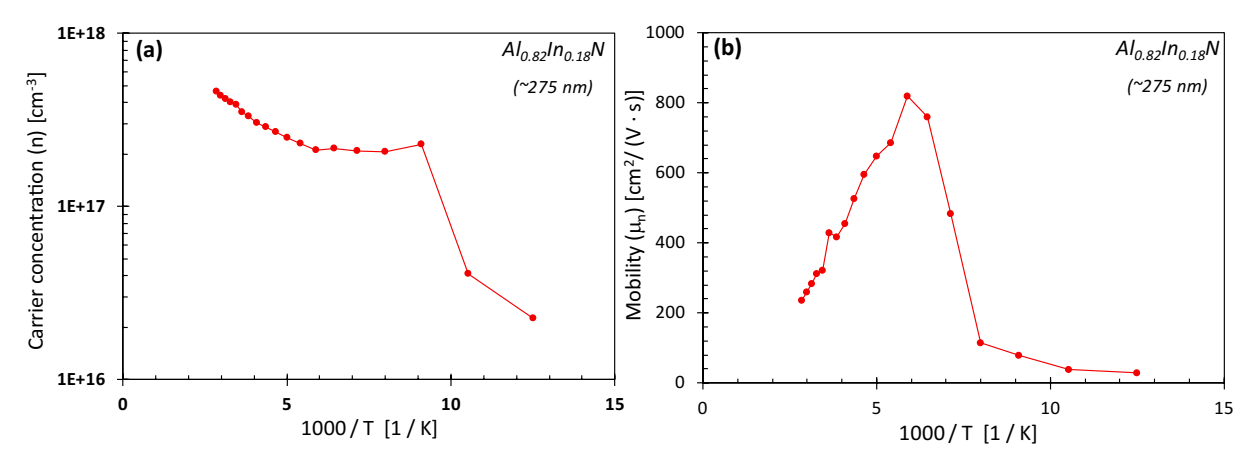


Fig. 3. (a) Electron concentration and (b) mobility plotted as functions of 1000/Temperature (T) for the Al_{0.82}In_{0.18}N sample grown on u-GaN, for temperatures varying from 80 K up to 350 K.

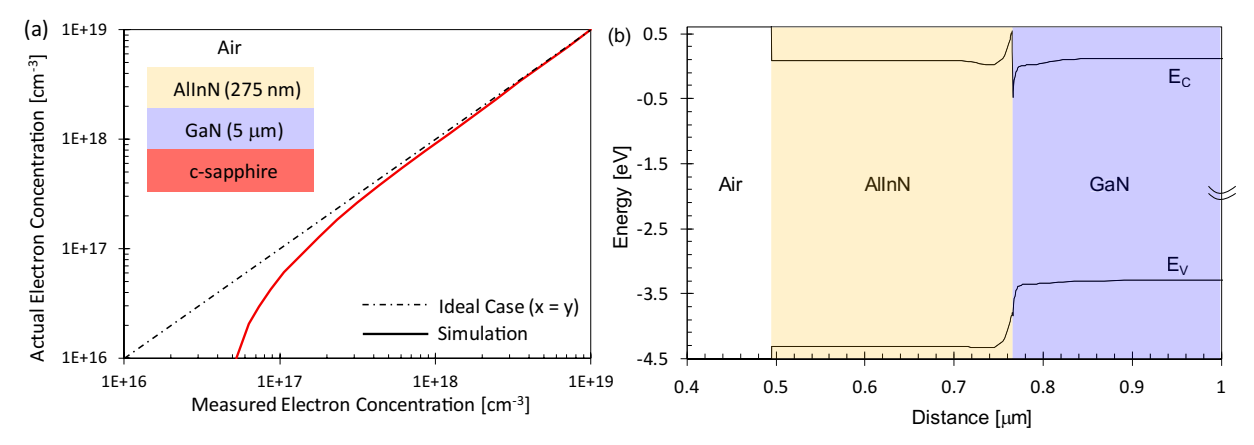


Fig. 4. . (a) Plot of actual electron concentration versus the measured electron concentration obtained from TCAD simulations. The dotted line represents the case where no 2DEG contribution is present, while the straight is with the 2DEG contribution. (b) Energy band diagram of the simulated structure, where the shaded areas represent the AlInN and GaN layers, respectively.

growing on free-standing (FS) GaN substrates the impurity incorporation and defect density could be significantly reduced and may thus lead to even lower background doping densities on the order of $\sim 10^{16}$ cm⁻³. Secondary ion mass spectroscopy (SIMS) measurements performed on the AlInN samples and the analysis (data not shown) indicated very low Si concentrations ($\sim 10^{17}$ atoms/cm $^{-3}$), that is closely matched to the measured background carrier concentration. Additionally, the SIMS results show a Si spike at the AlInN/GaN interface, indicating that the initial stage of the growth is influenced by the exposure of the u-GaN to ambient air, resulting in Si accumulation at the surface [32]. Moreover, other studies have pointed out that oxygen is omnipresent during growth and tends to saturate at a level of $\sim 10^{19}$ atoms/cm⁻³, similar to what we observe in our sample. Carbon levels, on the other hand, are more prone to growth conditions and can be controlled to achieve values of $\sim 10^{18}$ atoms/cm⁻³ [29]. It is also important to note that the reduction in the background carrier concentration may be related to our improved growth conditions, as similar studies in Ref. [29] have shown the relation of the carbon and oxygen incorporation as a function of reactor pressure, deeming the ~75 Torr as possibly ideal for the growth of AlInN. Although the effect of the optimized growth conditions, as compared to our previous works in Ref. [23], is still relatively unknown, it is possible that the reactor conditioning and preparation may also play a role in improving the overall material quality and should therefore be closely monitored in future experiments. Thus, going forward, one of the important aspects towards achieving AlInN films with even lower background doping densities will require lowering the carbon and silicon levels in the film, while carefully optimizing the reactor for the growth of the AlInN semiconductor.

4. Conclusion

The growth of ~275 nm thick AlInN films nearly lattice-matched to GaN (on sapphire) via MOVPE is reported. The structural and morphological characteristics determined by XRD and AFM measurements show relatively smooth surfaces. Spectroscopic ellipsometry measurements provide refractive index, extinction coefficient and absorption spectra that are similar to previous reports. In addition, temperature-dependent Hall measurements in the Van der Pauw configuration show low background doping densities with a room-temperature $n \sim 3 \times 10^{17}~{\rm cm}^{-3}$ and a mobility of $\mu_n \sim 320~{\rm cm}^2/{\rm V}\cdot{\rm s}$. Moreover, TCAD simulations of the grown structure show that the influence of the 2DEG arising from the GaN/AlInN interface on the Hall-measured carrier concentration are minimal. Thus, our results indicate the promising potential of careful growth optimization for achieving high-quality AlInN films with low surface roughness and low background

doping densities. Such AlInN films are interesting for the next-generation, III-nitride-based power devices.

Declaration of Competing Interest

The authors declare that they have no known competing financial interests or personal relationships that could have appeared to influence the work reported in this paper.

Acknowledgements

The work is supported by US National Science Foundation (DMR 1505122, DMR 1708227, DMR 1726395, and ECCS 1935295), and the Daniel E. '39 and Patricia M. Smith Endowed Chair Professorship Fund.

References

- [1] S. Nakamura, G. Fasol (Eds.), The Blue Laser Diode, Springer-Verlag, Berlin, 1997.
- [2] H. Harima, Properties of GaN and related compounds studied by means of Raman scattering, J. Phys.: Condens. Matter. 14 (2002) R967-R993.
- [3] G. Zeng, C.K. Tan, N. Tansu, B.A. Krick, Ultralow wear of gallium nitride, Appl. Phys. Lett. 109 (2016) 051602.
- [4] http://www.nobelprize.org/nobel_prizes/physics/laureates/2014/.
- [5] J.Y. Tsao, et al., Ultrawide-bandgap semiconductors: research opportunities and challenges, Adv. Electron. Mater. 4 (2017) 1600501.
- [6] J.B. Varley, A. Janotti, C. Franchini, C.G. Van de Walle, Role of self-trapping in luminescence and p-type conductivity of wide-band-gap oxides, Phys. Rev. B 86 (2012) 081109(R).
- [7] J.-F. Carlin, et al., Progresses in III-nitride distributed Bragg reflectors and microcavities using AlInN/GaN materials, Phys. Stat. Solidi (b) 242 (2005) 11.
- [8] A. Castiglia, et al., Blue laser diodes including lattice-matched Al0.83In0.17N bottom cladding layer, Electron. Lett. 44 (2008) 8.
- [9] Y. Sakai, T. Morimoto, T. Egawa, T. Jimbo, Metal organic chemical vapor deposition growth and characterization of AlInN-based Schottky ultraviolet photodiodes on AlN template, Jpn. J. Appl. Phys. 50 (2011) 01AD01.
- [10] E. Kohn, F. Medjdoub, InAlN a new barrier material for GaN-based HEMTs, Proc. 14th Int. Work. Phys. Semic. Dev., IWPSD 6 (2007) 311–316.
- [11] Q. Fareed, et al., High voltage operation of field-played AlInN HEMTs, Phys. Status Solidi Curr. Top. Solid State Phys. 8 (7–8) (2011) 2454–2456.
- [12] W. Sun, S.A. Al Muyeed, R. Song, J.J. Wierer Jr., N. Tansu, Integrating AlInN interlayers into InGaN/GaN multiple quantum wells for enhanced green emission, Appl. Phys. Lett. 112 (2018) 201106.
- [13] J. Zhang, H. Tong, G. Liu, N. Tansu, High-temperature characteristics of Seebeck coefficients for AlInN alloys grown by metalorganic vapor phase epitaxy, J. Appl. Phys. 110 (2011) 4.
- [14] H. Tong, et al., Thermoelectric properties of lattice-matched AlinN alloy grown by metal organic chemical vapor deposition, Appl. Phys. Lett. 97 (2010) 112105.
- [15] Y. Taniyasu, J.-F. Carlin, A. Castiglia, R. Butté, N. Grandjean, Mg doping for p-type AlInN lattice-matched to GaN, Appl. Phys. Letters 101 (2012) 082113.
- [16] K. Ikeyama, et al., Room-temperature continuous-wave operation of GaN-based vertical-cavity surface-emitting lasers with n-type conducting AlInN/GaN distributed Bragg reflectors, Appl. Phys. Express 9 (2016) 10.
- [17] M. Peart, et al., Thermal oxidation of AlInN for III-nitride electronic and optoelectronic devices, ACS Appl. Electron. Mater. 1 (2019) 8.
- [18] D. Borovac, W. Sun, R. Song, J.J. Wierer Jr., N. Tansu, On the thermal stability of

- nearly lattice-matched AlInN films grown on GaN via MOVPE, J. Crys. Growth 533 (2020) 125469.
- [19] M. Peart, N. Tansu, J.J. Wierer Jr., AlInN for vertical power electronic devices, IEEE Trans. Elec. Devices 65 (2018) 10.
- [20] G. Perillat-Merceroz, G. Cosendey, J.-F. Carlin, R. Butté, N. Grandjean, Intrinsic degradation mechanism of nearly lattice-matched InAlN layers grown on GaN substrates, J. Appl. Phys. 113 (2013) 063506.
- [21] M. Miyoshi, M. Yamanaka, T. Egawa, T. Takeuchi, Microstructure variation in thick AlInN films grown on c-plane GaN on sapphire by metalorganic chemical vapor deposition, J. Cryst. Growth 506 (2019) 40–44.
- [22] G. Parish, S. Keller, S.P. DenBaars, U.K. Mishra, SIMS Investigations into the effect of growth conditions on residual impurity and silicon incorporation in GaN and AlxGa1-xN, J. Elec. Mater. 29 (2000) 1.
- [23] G.Y. Liu, et al., Metalorganic vapor phase epitaxy and characterizations of nearly-lattice-matched AlInN alloys on GaN/sapphire and free-standing GaN substrates, J. Cryst. Growth 340 (2012) 66–73.
- [24] Z.L. Miao, et al., Strain effects on InxAl1-xN crystalline quality grown on GaN templates by metalorganic chemical vapor deposition, J. Appl. Phys. 107 (2010) 043515.
- [25] G. Cosendey, J.-F. Carlin, N.A.K. Kaufmann, R. Butté, N. Grandjean, Strain

- compensation in AlInN/GaN multilayers on GaN substrates: applications to the realization of defect-free Bragg reflectors, Appl. Phys. Lett. 98 (2011) 181111.
- [26] T. Aschenbrenner, et al., Optical and structural characterization of AlInN layers for optoelectronic applications, J. Appl. Phys. 108 (2010) 063533.
- [27] S. Shishehchi, F. Bertazzi, E. Bellotti, A numerical study of low- and high-field carrier transport properties in In_{0.18}Al_{0.82}N lattice-matched to GaN, J. Appl. Phys. 113 (2013) 203709.
- [28] A. Sztein, J.E. Bowers, S.P. DenBaars, S. Nakamura, Thermoelectric properties of lattice matched InAlN on semi-insulating GaN templates, J. Appl. Phys. 112 (2012) 083716
- [29] R.B. Chung, et al., Growth study and impurity characterization of AlxIn1-xN grown by metal organic chemical vapor deposition, J. Cryst. Growth 324 (2012) 163–167.
- [30] M.A. Py, L. Lugani, Y. Taniyasu, J.-F. Carlin, N. Grandjean, Capacitance behavior of InAlN Schottky diodes in presence of large concentrations of shallow and deep states related to oxygen, J. Appl. Phys. 117 (2015) 185701.
- [31] S.L. Chuang, Physics of Photonic Devices, second ed., John Wiley & Sons Inc., Hoboken, New Jersey, 2009.
- [32] G. Koblmuller, R.M. Chu, A. Raman, U.K. Mishra, J.S. Speck, High-temperature molecular beam epitaxial growth of AlGaN/GaN on GaN templates with reduced interface impurity levels, J. Appl. Phys. 107 (2010) 043527.